HHS Public Access

Author manuscript

Magn Reson Med. Author manuscript; available in PMC 2019 February 01.

Published in final edited form as:

Magn Reson Med. 2018 February ; 79(2): 815–825. doi:10.1002/mrm.26742.

Quantitative Single Breath-Hold Renal Arterial Spin Labeling Imaging at 7T

Xiufeng Li[1,*], **Edward J. Auerbach**[1], **Pierre-Francois Van de Moortele**[1], **Kamil Ugurbil**[1], and **Gregory J. Metzger**[1]

[1]Center for Magnetic Resonance Research, University of Minnesota, Minneapolis, United States

Abstract

Purpose—To evaluate the feasibility of quantitative single breath-hold renal arterial spin labeling (ASL) imaging at 7T.

Methods—A single-shot fast spin echo FAIR method was used to perform two studies. First, a multi-delay perfusion study was performed to estimate the spin labeling temporal bolus width achievable with a local transceiver array coil at 7T. Second, with a conservatively defined bolus width, a quantitative perfusion study was performed using the single subtraction approach. To address issues of B_1^+ inhomogeneity/efficiency and excessive short-term specific absorption rates, various strategies were employed, such as dynamic RF shimming and optimization.

Results—A conservative temporal bolus width of 600 ms determined from the multi-delay study was applied for single-subtraction imaging to measure the renal blood flow in the cortex and medulla: 303 ± 31.8 and 91.3 ± 15.2 (mL/100 g/min), respectively. The estimated spatial and temporal signal-to-noise ratios of renal perfusion measurements were 3.8 ± 0.7 and 2.4 ± 0.6 for the cortex, and 2.2 ± 0.6 and 1.4 ± 0.2 for the medulla.

Conclusion—With proper management of field strength specific challenges, quantitative renal ASL imaging can be achieved at 7T within a single breath-hold.

Keywords

magnetic resonance imaging (MRI); arterial spin labeling (ASL); renal perfusion or renal blood flow (RBF); kidneys; ultra-high field (UHF); and 7T

INTRODUCTION

Without the risk of ionizing radiation and the need for contrast agents, renal ASL imaging is a well-suited perfusion imaging approach for the assessment of renal dysfunction (1,2) and complications following renal transplantation (3,4). However, due to the intrinsically low signal-to-noise ratio (SNR) of ASL imaging, long acquisition times are needed to accommodate signal averaging at clinical field strength (up to 3T) which makes ASL imaging susceptible to artifacts resulting from physiologic motion (4). At ultra high field

[*]Address correspondence: Xiufeng Li, Ph.D., Center for Magnetic Resonance Research, University of Minnesota - Twin Cities, 2021 6th St. SE, Minneapolis, MN 55455, Tel: 612-625-7872, Fax: 612-626-2004, lixx1607@umn.edu.

[*]Presented in parts at the ISMRM 21st Annual Meeting & Exhibition, Salt Lake City, Utah, USA

(UHF, ≥7T), there is a strong potential to reduce image acquisition times and minimize motion-associated artifacts (5,6) due to increased SNR, prolonged longitudinal relaxation times of arterial blood (7) and renal tissue (8), and improved parallel imaging performance (9).

Well-known challenges also exist to performing MRI at 7T. With the increase of magnetic field strength from 3T to 7T, the susceptibility induced inhomogeneity of the B_0 field increases which will increase image distortion and signal loss especially for fast imaging sequences such as echo planar imaging (EPI) (10). In addition, the RF wavelength becomes shorter resulting in constructive and destructive interferences of both the magnetic and electric fields causing decreased B_1+ efficiency and homogeneity while increasing local power deposition as measured by the specific absorption rate (SAR) (11,12).

In addition to these general challenges, successfully performing ASL imaging in the kidneys at 7T requires specific issues to be addressed. For example, RF pulses in the ASL sequence target different anatomical regions, having varied requirements with respect to B_1^+ amplitude, homogeneity and spatial coverage. As a result, optimizing the RF (i.e. B_1^+ shimming) using a single solution based on the target anatomy alone (i.e. the kidneys) is not sufficient (13). Furthermore, in contrast to studies at 3T, where the whole body coil is used for RF transmission, studies at 7T use local transceiver coils, which have limited B_1^+ coverage producing smaller temporal bolus widths that need to be estimated in order to achieve proper renal blood flow (RBF) quantification.

The purpose of this study is to present multiple strategies to address both field and method specific challenges and demonstrate the feasibility of quantitative single breath-hold renal ASL perfusion imaging at 7T.

METHODS

Subjects

A total of 12 healthy subjects were recruited for renal perfusion imaging studies at 7T. Imaging studies were performed after subjects provided written informed consent to participate in an institutional review board approved protocol. Five subjects (three males, 48 ± 27 years, and two females, 44 ± 16 years, mean ± standard deviation (S.D.)) took part in a study to determine the temporal bolus width achievable when using a local transceiver array coil, and seven subjects (four males, 32 ± 6 years, and three females, 47 ± 12 years, mean ± standard deviation (S.D.)) participated in a second study to measure quantitative renal perfusion using the single-subtraction approach (details of both studies are provided below).

MRI

MRI studies were performed on a Siemens 7T whole body MRI scanner with a 58 cm diameter bore, using a 16-channel transceiver stripline array driven by sixteen 1kW amplifiers (CPC, Pittsburgh, PA) (9). The 16-channel transceiver array coil consists of two plates with each having 8 stripline elements. The length of the stripline elements along the head-foot direction is 15 cm (9). These two plates were positioned around the abdomen to cover the kidney region anteriorly and posteriorly. The forward and reflected RF power from

each channel was monitored separately and continuously using a home-built power monitoring system (14). The time averaged power limits for each channel were set based on electromagnetic simulation results (9) and according to the International Electrotechnical Commission guidance document (15).

The imaging protocol included the acquisition of localizers using gradient recalled echo (GRE) imaging in three orthogonal orientations (sagittal, oblique coronal and axial), imaging acquisitions for B_0 and B_1^+ optimization, and renal perfusion imaging scans. To minimize the impact of physiological motion, each of the imaging acquisitions was performed during a single breath-hold on expiration. This includes the optimization of static magnetic fields within the imaging slice, achieved by performing B_0 shimming utilizing volumetric phase maps (8).

Renal Perfusion Imaging Sequences

Renal perfusion imaging studies used a flow-sensitive alternating inversion recovery (FAIR) method (16) for labeling and a single-shot fast spin echo (ss-FSE) method as the perfusion imaging readout, referred to as FAIR ss-FSE. The sequence diagram and relative spatial locations of each RF pulse in the sequence are illustrated in Figure 1.

As shown in Figure 1A, a single ss-FSE image is first acquired to measure the fully relaxed renal tissue magnetization (referred to as the M_0 image) prior to the acquisition of label and control images. The FAIR ss-FSE sequence consists of a pre-saturation RF pulse targeting the location and extent of the oblique coronal imaging slice followed by an inversion RF pulse centered on the coronal imaging slice but alternating between a small inversion slab for the control images and a large inversion slab for label images, Figure 1B. This labeling is followed by saturation RF pulses targeting a slab anterior and parallel to the imaging slice. The anterior saturation pulses are applied at a specified delay time (TI_1 in Figure 1A) after the inversion RF pulse to define the temporal bolus width of the labeled spins and are similar to the inferior saturation RF pulses of the QUIPSS II or Q2TIPS methods used in the brain (17,18). After the saturation RF pulses and before image acquisition, there is a post-bolus delay (TI-TI_1, Figure 1A) to allow the labeled blood time to travel down the vascular tree into the small arterioles and minimize the undesired hyper-intense intravascular signals. The time between the inversion RF pulse and image acquisition is referred to as the total delay time (TI). To minimize the peak amplitude of the inversion pulse, an optimized HS4 adiabatic pulse with a 20 ms duration and a time-bandwidth product of 20 was used (19). The ss-FSE imaging method was selected for image acquisition to better handle B_0 inhomogeneity thus avoiding the associated susceptibility artifacts present with echo planar imaging (EPI) methods (10), the standard readout used in the brain. To reduce RF power deposition from the ss-FSE readout, variable-rate selective excitation (VERSE) RF pulses (20) were used for refocusing as was a hyperecho phase and amplitude modulation scheme (21). Within each ASL scan, a noise image was acquired at the end of the acquisition by turning off RF pulses to facilitate perfusion SNR analysis. (22).

B_1^+ Management

Each RF pulse in the FAIR ss-FSE acquisition has different requirements in terms of homogeneity and efficiency, as well as spatial location and extent in the body (Figure 1). It is demonstrated that B_1^+ optimization using B_1^+ shimming for the target anatomy alone is not sufficient for renal ASL imaging (6). Therefore, in this application, B_1^+ optimization was achieved by dynamically applying different B_1^+ shimming solutions to satisfy the unique requirements of each pulse in the sequence (23).

The dynamic B_1^+ shimming strategy consisted of 2 solutions. The RF pulses for pre-saturation and the ss-FSE readout were specifically optimized in a region covering both kidneys while the anterior saturation and inversion RF pulses were optimized in a region covering both the descending aorta and the renal arteries. The regions of interest (ROIs) for B_1^+ shimming in the kidneys and that for B_1^+ shimming of the feeding arteries are indicated by green and red contours in Figure 2A, respectively.

The B_1^+ optimizations utilized a phase-only B_1^+ shimming approach based on the data acquired from a single small flip angle calibration scan consisting of three imaging slices (Figure 1B) obtained in a single breath-hold (13). The B_1^+ optimizations focused on a tradeoff between RF efficiency and B_1^+ field homogeneity (8). To minimize artifacts due to pulsatile flow in the arteries, the calibration scan utilized flow compensation gradients in both the slice and readout directions.

Following B_1^+ optimization in each region, two-dimensional flow compensated actual flip-angle imaging (AFI) (24) was performed to obtain relative B_1^+ maps with an imaging resolution of $2 \times 2 \times 5$ mm^3 (8). To correct the bias in B_1^+ estimation due to the imperfect 2D slice excitation profile, a previously determined scale factor was applied (8). Using the corrected 2D AFI results, the RF power for the final ASL acquisition was adjusted taking into account the relative efficiency between the two B_1^+ shimming solutions used in the two target regions.

After B_1^+ shimming and calibration, there exists a subject-dependent spatial variability in B_1^+. To minimize the effects of this inhomogeneous B_1^+ on inversion and thus labeling efficiency, a nominal flip angle (or an RF transmit voltage) at least two times that needed for an adiabatic inversion was consistently applied for the inversion RF pulse (19). Such a strategy ensured the adiabatic condition was achieved for the inversion RF pulse throughout nearly the entire labeling region. A conservative value of inversion efficiency, 0.95, was assumed for the studies performed with this strategy (Please refer to Supporting Figure S2 in the online supporting information document).

Before renal ASL imaging, a table of phases and gains determined from B_1^+ shimming were loaded into the system phase and gain controller (CPC, Pittsburgh, PA). The order of the solutions in the table was dictated by the B_1^+ shims needed for each successive RF pulse in the sequence. Dynamic shimming was made possible by programming the sequence with a TTL pulse before each RF pulse which triggers the phase and gain controller to increment to the next solution in the table thus loading the RF pulse specific B_1^+ shim. The table repeats

for each repetition of the sequence. The switching is nearly instantaneous, and takes approximately 10 μs.

Renal Perfusion Studies

Two renal perfusion imaging studies were performed: 1) a multi-delay perfusion study using varied total delay times to estimate temporal bolus widths, arterial transit times and RBF without applying anterior saturation RF pulses; and 2) an RBF quantification study using a single-subtraction approach with a fixed temporal bolus width and a single delay time (17,18).

The maximum achievable temporal bolus width in a given anatomy is limited by the extent of the RF field produced by the local transceiver array coil. However, within a target anatomy, there is a range of temporal bolus widths depending on the path and complexity of the vascular supply. For correct perfusion quantification using the single subtraction technique, the sequence prescribed temporal bolus width (TI_1) must be less than or equal to the shortest temporal bolus width achieved for imaged tissue, which can be determined by the multi-delay study.

Acquisition parameters for the multi-delay study included the following: TR/TE = 3500–4000/16 ms, hyper echo flip angle = 90°, FOV = 256 × 256, matrix size = 128 × 128, in-plane resolution = 2 × 2 mm^2, phase encoding direction = left to right with 50–80% oversampling and corresponding echo train length 28 – 32, slice thickness = 5 mm, partial Fourier = 5/8, GRAPPA parallel acceleration factor (R) = 4 with 24 separately acquired reference lines, total delay times (TI) = {0.3, 0.6, 0.9, 1.2, 1.5, 1.8, 2.1} s, control/label inversion slab size 25/160 mm, and the pairs of label and control images = 4. In this study, the anterior saturation RF pulses used for temporal bolus definition were disabled and the order of post-labeling delay times was randomized for each subject.

The single-subtraction study was performed with four pairs of label and control images using the same parameters as described above except that a fixed 600 ms temporal bolus width was applied with a 600 ms post-bolus delay. The selection of a 600 ms temporal bolus width was based on the multi-delay study results, which suggested that the temporal bolus width achieved with the applied body coil was consistently larger than 600 ms. The bolus width was defined by performing four saturation RF pulses on the anterior side of imaging slice after ASL inversion over a 50 ms interval and using a 60 mm slab (Figure 1B). To avoid intravascular artifacts, a post-bolus delay longer than the estimated longest arterial transit time was applied (please refer to Results and Discussion sections). Within the same perfusion acquisition, one noise image was also acquired after the ASL image acquisition by turning off all RF pulses.

Both the multi-delay and single subtraction studies were performed during a single breath-hold (6). The total acquisition time for a complete perfusion scan with M_0 and noise images may be as long as 40 s when using a 4 s TR, but the breath-hold duration was reduced to about 33 s by using the following strategy. Subjects were instructed to hold their breath only during the acquisition of the first M_0 image and the following 4 pairs of label and control images. As the M_0 image had no ASL preparation and associated total delay time, its

contribution to the total acquisition time was much shorter than that for a perfusion image and consisted of the ss-FSE readout time (114 to 130 ms for 50 to 80% phase oversampling) plus the time (T_d in Figure A) between this readout and the first ASL preparation. In addition, the subjects were instructed to resume their respiration once the acquisition of the last perfusion image was completed, which means breath-holding was not required during the T_d of the last perfusion image acquisition nor during the noise image acquisition. It is worth noting that it is not necessary to have subjects hold their breath during the noise image acquisition since all RF pulses were turned off in order to measure the thermal noise of the system. Therefore, the total duration of the breath-hold was equal to the total acquisition time for perfusion label and control images (8 measurements) plus the ss-FSE readout time for M_0.

Image Processing and Data Analysis

Post-processing was performed using SPM (Functional Imaging Laboratory, University College London, London, UK) including motion correction to address small drifts during the breath-hold. After motion correction for each renal ASL imaging scan, label and control images were first pair-wise subtracted to obtain four perfusion-weighted images that were subsequently averaged to get a mean perfusion-weighted image. By using the M_0 image as the reference, a mean normalized perfusion-weighted image representing the percent perfusion signal was calculated.

ROI-based analyses were performed in Matlab (MathWorks, Natick, MA, USA). The ROIs for the renal cortex and medulla were manually defined on the mean normalized perfusion-weighted images. In particular, for the multi-delay study, the ROIs were conservatively drawn on the mean normalized perfusion-weighted image acquired with a 0.6 s delay which best demonstrated the location of high intravascular signals which need to be avoided. To further reduce the impact of subtraction errors resulting from residual physiologic motion and intravascular perfusion signals, trimmed mean signals within ROIs were used in the final perfusion signal measurements by excluding the 5% of voxels with the lowest and highest values (25,26).

To estimate the temporal bolus width, arterial transit time and RBF using the renal perfusion signal from the multi-delay study, iterative nonlinear least-square model-fitting was performed to fit ASL signals to the three-phase, single-compartment model (27):

$$\Delta M(t)=0, \quad 0<t<\Delta t \quad [1]$$

$$\Delta M(t)=2\alpha \times M_{0b} \times RBF \times (t-\Delta t) \times \exp(-t/T_{1b}), \ \Delta t<t<\tau+\Delta t \quad [2]$$

$$\Delta M(t)=2\alpha \times M_{0b} \times RBF \times \tau \quad \times \exp(-t/T_{1b}), \ \tau+\Delta t<t \quad [3]$$

where ΔM(t) is the mean of perfusion signal in a specified ROI at inversion time t, Δt the arterial transit time, τ the temporal bolus width, M_{0b} the fully relaxed magnetization of arterial blood, T_{1b} the longitudinal relaxation time of the arterial blood, 2041 ms (7), and α the labeling efficiency, assumed to be 0.95 for the applied HS4 adiabatic RF pulse (19). M_{0b} was estimated from the M_0 image and the renal blood–tissue partition coefficient λ (assumed to be 0.8 (28)):

$$\mathrm{M_{0b}}=\mathrm{M_0}/\lambda \quad [4]$$

The arterial transit time, RBF and temporal bolus width parameters were estimated from Eqs. [1] – [3].

For the perfusion study using the single-subtraction approach, RBF maps were obtained by applying the simplified single compartment model (29,30):

$$\mathrm{RBF\,(r)}=\Delta\mathrm{M\,(r)}/[2\alpha\times\mathrm{M_{0b}}\times\mathrm{TI_1}\times\exp\,(-\mathrm{TI}/\mathrm{T_{1b}})] \quad [5]$$

where r is the spatial location of imaging voxel, ΔM the perfusion signal, TI_1 the sequence-defined temporal bolus width, and TI the total delay time (Figure 1).

Spatial and temporal SNR analyses were performed for the single-subtraction perfusion study. The spatial perfusion SNR was estimated as the ratio of the mean perfusion signal to the noise within a defined ROI. The noise was estimated from the noise image using the following formula:

$$\sigma=stddev(S_N)\times\sqrt{2/(4-\pi)} \quad [6]$$

where σ represents estimated noise, S_N is the noise signal intensity within the cortex or medulla, *stddev* is the standard deviation of noise signal intensities, and $\sqrt{2}/(4-\pi)$ the correction factor to remove the bias due to assessing noise in a magnitude image (31). The temporal perfusion SNR was calculated within the regions of the cortex and medulla as the ratio of the mean perfusion signal obtained from the mean perfusion-weighted image to the mean of the temporal standard deviation map obtained across the four perfusion-weighted images.

Statistical analysis was performed in Excel (Microsoft Redmond, WA, USA) for within-group comparisons using a two-tailed paired t test or between-group comparisons using two-tailed two-sample t tests. Significance was determined if the P value was ≤ 0.05.

RESULTS

Compared to using a single B_1^+ shimming solution, dynamically applied multiple B_1^+ shimming solutions based on ROIs separately targeting the kidneys on the one hand, and their feeding arteries on the other hand, can improve renal perfusion imaging quality and

SNR. The relative B_1^+ maps using a tradeoff B_1^+ shim solution from regions covering either the kidneys or the feeding arteries separately are presented in Figures 2B–2C. In particular, using ROIs that only cover the feeding arteries can greatly improve the B_1^+ performance within this region, which resides deep in the body (Figure 2C). The perfusion-weighted image obtained using a single B_1^+ shim solution optimized over a single large ROI encompassing both the kidneys and feeding arteries, and that obtained using two dynamically applied B_1^+ shim solutions optimized on the two regions separately are shown in Figure 2D (Please refer to Supporting Figure S1 in the online supporting information document for quantitative comparisons of spatial and temporal SNRs between renal perfusion measurements with and without dynamically applied B_1^+ shimming solutions). With optimized B_1+ and B_0 fields, perfusion maps generated with increasing numbers of signal averages are shown in Figure 3.

Multi-delay perfusion imaging results of a single subject are presented in Figure 4, and the group means of dynamic perfusion signal from five subjects are shown in Figure 5. The estimated arterial transit time, temporal bolus width and RBF from five subjects are summarized in Table 1. All quantitative metrics were significantly different between the cortex and medulla based on the two-tailed paired t test. Arterial transit times ranged from ~80 ms to ~150 ms for renal cortex and ~180 ms to ~250 ms for renal medulla. Meanwhile, the temporal bolus width was consistently longer than 600 ms in the cortex and 700 ms in the medulla with the local transceiver RF coil used in this study.

Based on the multi-delay results, a fixed temporal bolus width of 600 ms was used in the single-subtraction renal perfusion imaging studies. The M_0 image, ROIs for cortical and medullary RBF quantification, RBF map and the acquired noise image of one subject from the single-subtraction perfusion study are shown in Figure 6. The RBF, spatial and temporal SNRs estimated using two, three and four pairs of label and control images (or averages) are presented in Table 2. The temporal SNR, a function of both system and physiologic stability, is consistently lower than spatial SNR and a major limiting factor with respect to obtaining reliable perfusion data. The statistical analyses indicate that the RBF measurements using two averages are significantly different from those using four averages, but no significant differences were observed between RBF calculated with three or four averages. While the increase in SNR is expected to be proportional to the square root of the number of averages, there is a trend towards lower SNR values, especially in the medulla, when going from three to four averages. This lower than expected temporal and spatial SNR may result from increased physiologic motions near the end of the breath-hold. Further analyses suggest no significant differences between the RBF values estimated from the more time-efficient single-subtraction study with a temporal bolus width of 600 ms using either three or four averages and those from the multi-delay study.

DISCUSSION

Although we expect that 7T will benefit ASL perfusion imaging based on previous simulations (5), well-known technical challenges needed to be overcome before such benefits could be realized and evaluated. The current study presents strategies for

overcoming the technical challenges and demonstrates, for the first time, the feasibility of obtaining quantitative non-contrast enhanced renal ASL perfusion imaging at 7T.

Strategies to Manage B_0 and B_1^+

The inhomogeneity of B_0 and B_1^+ becomes severe with the increase in magnetic field strength, and poses a critical technical challenge to performing UHF MRI. In the present study, multiple strategies have been utilized to address these issues. To address the static field inhomogeneity, B_0 shimming was performed by using 3D phase maps acquired within a single breath-hold (8). To further reduce image distortion and the susceptibility artifacts induced by B_0 inhomogeneity as observed in previous FAIR EPI study (10), ss-FSE was used as the imaging readout. To address the B_1^+ inhomogeneity, dynamically applied B_1^+ shimming solutions optimized on specific anatomic regions of interest were used to satisfy the specific needs of individual RF pulses in the imaging sequence. Even with the dynamically applied B_1+ shimming solutions separate for the imaging readout and ASL labeling, there still exists residual spatial variation in B_1^+, potentially impacting RBF quantification.

Regarding the imaging readout, while B_1^+ variability persists even after optimizing over the imaging volume, the potential impact on the perfusion quantification has been avoided by the acquisition and processing strategies applied. As observed, the B_1^+ field drops significantly within the kidneys posterior to anterior as expected given the increasing distance from the surface of the body array (Figure 2). Using an oblique coronal slice can reduce B_1^+ variation within the imaging slice, but the B_1^+ coefficient of variance was still as large as 25%. While the B_1^+ field variation with the imaging region results in an inhomogeneous perfusion signal and SNR, it will not affect the calculated perfusion values. This is because using an M_0 image acquired with the same B_1^+ solution can effective normalizes the impact of the B_1 fields of both the transmission and the reception. However, it should be noted that suboptimal B_1^+ for the FSE readout degrades perfusion SNR even if not impacting RBF quantification..

In terms of ASL labeling, although feasible, it remains challenging to achieve a sufficiently high B_1^+ amplitude to invert the spins over the entire labeling region. To increase the labeling efficiency, a smaller targeted ROI was used to cover the aorta and renal arteries for B_1^+ optimization instead of using an ROI to cover both the kidneys and vessels. This strategy effectively improved the transmit efficiency and allowed for increased B_1^+ magnitude and homogeneity, both of which improved renal perfusion image quality in terms of SNR (Figure 2) (Please refer to Supporting Figure S2 in the online supporting information document). In fact, the increased efficiency made it possible to use twice the nominal flip angle (or an RF transmit voltage) for the inversion RF in order to minimize the impact of the subject-dependent B_1^+ inhomogeneity. This strategy was accomplished while keeping the overall short-term SAR of the sequence around 90 to 95% of the limit and while using reasonable repetition times and breath-hold durations.

While the B_1^+ field generated by the applied coil extends beyond its 15 cm physical length, the field drops off quickly in the cranial-caudal directions. This limits the effective labeling size in the foot-head direction and thus the achievable temporal bolus width at 7T.

Therefore, the bolus width achieved at 7T is much smaller than that at 3T where all the blood in the body can be inverted in ASL labeling preparation. In general, a longer bolus width provides higher perfusion SNR, and this can only be realized if the labeled blood is allowed to substantially relax before the next ASL labeling preparation. Allowing the blood to fully relax would require longer TRs and decrease the advantage of the longer bolus width while increasing acquisition and breath hold times.

Optimization for Single-Subtraction Renal ASL Imaging

Proper selection of the sequence-defined temporal bolus width is essential for quantitative perfusion imaging using the single-subtraction approach. This becomes even more critical for 7T MRI studies when local transmit coils are used. To minimize the impact of subject-dependent variations in bolus widths, a conservatively short value, 600 ms, was chosen even though slightly longer bolus widths were observed in all individuals in the multi-delay studies for both the cortex and medulla.

The total delay time used in the single subtraction acquisitions was 1200 ms, which means that, in addition to the 600 ms temporal bolus width, a 600 ms post-bolus delay was applied. The reason to select a post-bolus delay time longer than the estimated arterial transit time (i.e. 110.1 ± 25.9 ms for the cortex and 206.8 ± 27.0 ms for the medulla, Table 1) is to minimize intravascular artifacts. In fact, it is the increased tissue and blood T_1 at 7T that allows such a long total delay time to be used for the single breath-hold acquisition without sacrificing significant perfusion signal SNR. Although intravascular effects can be managed with post processing strategies, it will nevertheless reduce RBF quantification reliability.

In the multi-delay model fitting, the blood T_1, instead of tissue T_1, was applied with the assumption that the labeled blood remained primarily within the vascular space and did not exchange into the renal tissue within the timeframe of the perfusion acquisition. Such an assumption is valid for the multi-delay measurements with short delay times. In particular, since the T_1 of the medulla (2094 ms) (8) is very close to that of the arterial blood (2041 ms) (7), using the blood T_1 for the model fitting of the measurements within the medulla will not present significant systematic errors. However, because the T_1 values of the blood and the cortex (1661 ms) (8) are significantly different, using either T_1 value for the model fitting in this region can result in significant systematic errors. Our results (please refer to Supporting Figure S3 in the online supporting information document) suggest that using blood T_1 may underestimate ATT, temporal bolus width and RBF within the cortex, while using the cortical T_1 may overestimate these parameters. Furthermore, our results suggest that the estimated temporal bolus widths in the cortex are consistently shorter than those in the medulla (Table 1) no matter which T_1 value is used. Therefore, in the cortical region, the blood T_1 was used for the multi-delay model fitting as it provides a conservative estimate of the temporal bolus width. With the same assumption, the blood T_1 was also used for RBF quantification for the single-subtraction studies.

Compared to the multi-delay experiment, the single-subtraction approach is much more efficient, and therefore will be preferred in future applications. While estimates of cortical and medullary RBF are comparable to those measured in previous studies at 3T (4,32,33),

renal perfusion imaging within a single breath-hold at 7T holds the promise of reduced motion sensitivity and increased quantification reliability.

Strategies to Comply with SAR Limits

Because of the high power deposition resulting from the inversion and refocusing RF pulses, the short-term SAR limit was found to be the dominant constraint when using the single breath-hold ss-FSE FAIR approach for renal ASL imaging. To manage the short-term SAR, several strategies were employed: 1) high parallel imaging acceleration factors (e.g., 4) and partial Fourier (e.g., 5/8) were used to reduce the FSE echo train length and thus the number of refocusing RF pulses; 2) reference lines for parallel imaging were acquired separately and once at the beginning of perfusion scan and before the acquisition of the M_0; 3) VERSE RF pulses and hyper-echoes were used within the ss-FSE imaging readout; and 4) in contrast to using a large overall ROI to optimize B_1^+, separate ROIs targeting specific RF pulse dependent anatomic regions were used to increase transmit efficiency. These strategies proved effective at minimizing short-term SAR, allowing perfusion imaging to be acquired in a single, albeit sometimes long, breath-hold.

Study Limitations

Although this study demonstrates that quantitative renal ASL perfusion imaging can be achieved within a single breath-hold at 7T, the current implementation has several limitations. First, the presented approach only allows single slice coverage while whole kidney coverage can be only achieved through multiple single breath-hold acquisitions. The prolonged longitudinal relaxation times of both arterial blood and renal tissue at 7T should allow more imaging slices to be acquired after a single ASL preparation, but the short-term SAR constraints currently make this impossible. Although multi-slice renal perfusion imaging using FAIR with an EPI readout has been previously demonstrated at 7T without SAR issues (10), this acquisition strategy yields inconsistent image quality and suffers from susceptibility based image distortion. Second, although our results suggest that comparable RBF estimates can be achieved using three, instead of four, pairs of label and control images, with a long repetition time (e.g., 4 s), the total breath-hold duration (e.g., about 25 s in some instances) can still make the current approach challenging for patients. Although it has been shown that 7T can improve the performance of parallel imaging (9), an acceleration factor 4 may result in a higher noise level than that at 3T where an acceleration factor of 2 is common. Third, constrained by the limited short-term SAR, it is impossible to perform background suppression (34) to further minimize subtraction errors due to residual physiologic motion for the single breath-hold renal perfusion studies at 7T. Therefore, a direct comparison with 3T is warranted to evaluate the benefits of 7T on renal ASL imaging.

Finally, while the multiple B_1^+ optimizations can address the specific needs of different RF pulses in the sequence, it unfortunately prolongs the total study time. Even though an improved labeling efficiency was achieved by separately optimizing the RF over the labeling vessels, quantification of overall labeling efficiency remains challenging and was not measured in the current study for each subject. Evaluating this metric and assessing the subsequent errors in RBF quantification would be important prior to using such a method in clinical studies.

To make UHF renal ASL imaging a useful tool for clinical research, further technical developments are needed. For example, both alternative adiabatic RF pulses (e.g., gradient offset independent adiabatic (GOIA) RF pulse (19)) and imaging readouts with lower total RF power requirements can decrease repetition times and therefore the duration of the breath hold. Recent studies have also demonstrated that 7T body imaging with array coils using alternative design (e.g., antenna coil) can provide greater transmit efficiency and SAR performance (35,36), which will benefit both ASL labeling and kidney imaging with reduced power deposition. Furthermore, the application of parallel transmit RF pulses with designs that can simultaneously minimize the B_1^+ inhomogeneity and reduce RF power deposition hold promise to even further improve UHF renal perfusion imaging (37).

Supplementary Material

Refer to Web version on PubMed Central for supplementary material.

Acknowledgments

This study was supported by National Institute of Health P41 EB015894, RR026783, S10 RR026783, and University of Minnesota Foundation (UMF0003900). Research reported in this publication was also supported by the National Center for Advancing Translational Sciences of the National Institutes of Health Award UL1TR000114. The content is solely the responsibility of the authors and does not necessarily represent the official views of the National Institutes of Health.

References

1. Pedrosa I, Alsop DC, Rofsky NM. Magnetic resonance imaging as a biomarker in renal cell carcinoma. Cancer. 2009; 115(10 Suppl):2334–2345. [PubMed: 19402070]
2. Dong J, Yang L, Su T, Yang X, Chen B, Zhang J, Wang X, Jiang X. Quantitative assessment of acute kidney injury by noninvasive arterial spin labeling perfusion MRI: a pilot study. Sci China Life Sci. 2013; 56(8):745–750. [PubMed: 23740361]
3. Heusch P, Wittsack HJ, Blondin D, Ljimani A, Nguyen-Quang M, Martirosian P, Zenginli H, Bilk P, Kropil P, Heusner TA, Antoch G, Lanzman RS. Functional evaluation of transplanted kidneys using arterial spin labeling MRI. Journal of magnetic resonance imaging: JMRI. 2014; 40(1):84–89. [PubMed: 24123319]
4. Artz NS, Sadowski EA, Wentland AL, Grist TM, Seo S, Djamali A, Fain SB. Arterial spin labeling MRI for assessment of perfusion in native and transplanted kidneys. Magnetic resonance imaging. 2011; 29(1):74–82. [PubMed: 20850241]
5. Li, X., Ugurbil, K., Metzger, GJ. Theoretical Evaluation of Ultra High Field Benefits to Non-contrast Enhanced Renal Perfusion Imaging Using FAIR-EPI. Proceedings of the 20th Annual Meeting of ISMRM; Salt Lake City, USA. 2013; Abstract 1540
6. Li, X., Snyder, CJ., Van de Moortele, P-F., Ugurbil, K., Metzger, GJ. Feasibility of Single Breath-hold Renal Perfusion Imaging at 7T. Proceedings of the 20th Annual Meeting of ISMRM; Salt Lake City, USA. 2013; Abstract 0030
7. Kalavagunta C, Michaeli S, Metzger GJ. In vitro Gd-DTPA relaxometry studies in oxygenated venous human blood and aqueous solution at 3 and 7 T. Contrast Media Mol Imaging. 2014; 9(2): 169–176. [PubMed: 24523062]
8. Li X, Bolan PJ, Ugurbil K, Metzger GJ. Measuring renal tissue relaxation times at 7 T. NMR in biomedicine. 2015; 28(1):63–69. [PubMed: 25346367]
9. Snyder CJ, Delabarre L, Moeller S, Tian J, Akgun C, Van de Moortele PF, Bolan PJ, Ugurbil K, Vaughan JT, Metzger GJ. Comparison between eight- and sixteen-channel TEM transceive arrays for body imaging at 7 T. Magnetic resonance in medicine: official journal of the Society of Magnetic Resonance in Medicine/Society of Magnetic Resonance in Medicine. 2012; 67(4):954–964.

10. Li, X., Snyder, C., Van de Moortele, P-F., Ugurbil, K., Metzger, GJ. Non-Contrast Enhanced Human Renal Perfusion Imaging Using Arterial Spin Labeling at 7 T: Initial Experience. Proceedings of the 20th Annual Meeting of ISMRM; Melbourne, Australia. 2012; Abstract 1310
11. Vaughan JT, Snyder CJ, DelaBarre LJ, Bolan PJ, Tian J, Bolinger L, Adriany G, Andersen P, Strupp J, Ugurbil K. Whole-body imaging at 7T: preliminary results. Magnetic resonance in medicine: official journal of the Society of Magnetic Resonance in Medicine/Society of Magnetic Resonance in Medicine. 2009; 61(1):244–248.
12. Vaughan JT, Garwood M, Collins CM, Liu W, DelaBarre L, Adriany G, Andersen P, Merkle H, Goebel R, Smith MB, Ugurbil K. 7T vs. 4T: RF power, homogeneity, and signal-to-noise comparison in head images. Magnetic resonance in medicine: official journal of the Society of Magnetic Resonance in Medicine/Society of Magnetic Resonance in Medicine. 2001; 46(1):24–30.
13. Metzger GJ, Snyder C, Akgun C, Vaughan T, Ugurbil K, Van de Moortele PF. Local B1+ shimming for prostate imaging with transceiver arrays at 7T based on subject-dependent transmit phase measurements. Magnetic resonance in medicine: official journal of the Society of Magnetic Resonance in Medicine/Society of Magnetic Resonance in Medicine. 2008; 59(2):396–409.
14. Metzger GJ, van de Moortele PF, Akgun C, Snyder CJ, Moeller S, Strupp J, Andersen P, Shrivastava D, Vaughan T, Ugurbil K, Adriany G. Performance of external and internal coil configurations for prostate investigations at 7 T. Magnetic resonance in medicine: official journal of the Society of Magnetic Resonance in Medicine/Society of Magnetic Resonance in Medicine. 2010; 64(6):1625–1639.
15. Dixon WT, Du LN, Faul DD, Gado M, Rossnick S. Projection angiograms of blood labeled by adiabatic fast passage. Magnetic resonance in medicine: official journal of the Society of Magnetic Resonance in Medicine/Society of Magnetic Resonance in Medicine. 1986; 3(3):454–462.
16. Kim SG, Tsekos NV. Perfusion imaging by a flow-sensitive alternating inversion recovery (FAIR) technique: application to functional brain imaging. Magnetic resonance in medicine: official journal of the Society of Magnetic Resonance in Medicine/Society of Magnetic Resonance in Medicine. 1997; 37(3):425–435.
17. Wong EC, Buxton RB, Frank LR. Quantitative imaging of perfusion using a single subtraction (QUIPSS and QUIPSS II). Magnetic resonance in medicine: official journal of the Society of Magnetic Resonance in Medicine/Society of Magnetic Resonance in Medicine. 1998; 39(5):702–708.
18. Luh WM, Wong EC, Bandettini PA, Hyde JS. QUIPSS II with thin-slice TI1 periodic saturation: a method for improving accuracy of quantitative perfusion imaging using pulsed arterial spin labeling. Magnetic resonance in medicine: official journal of the Society of Magnetic Resonance in Medicine/Society of Magnetic Resonance in Medicine. 1999; 41(6):1246–1254.
19. Garwood M, DelaBarre L. The return of the frequency sweep: designing adiabatic pulses for contemporary NMR. J Magn Reson. 2001; 153(2):155–177. [PubMed: 11740891]
20. Hargreaves BA, Cunningham CH, Nishimura DG, Conolly SM. Variable-rate selective excitation for rapid MRI sequences. Magnetic resonance in medicine: official journal of the Society of Magnetic Resonance in Medicine/Society of Magnetic Resonance in Medicine. 2004; 52(3):590–597.
21. Hennig J, Scheffler K. Hyperechoes. Magnetic resonance in medicine: official journal of the Society of Magnetic Resonance in Medicine/Society of Magnetic Resonance in Medicine. 2001; 46(1):6–12.
22. Li X, Wang D, Auerbach EJ, Moeller S, Ugurbil K, Metzger GJ. Theoretical and experimental evaluation of multi-band EPI for high-resolution whole brain pCASL Imaging. NeuroImage. 2015; 106:170–181. [PubMed: 25462690]
23. Metzger GJ, Auerbach EJ, Akgun C, Simonson J, Bi X, Ugurbil K, van de Moortele PF. Dynamically applied B1+ shimming solutions for non-contrast enhanced renal angiography at 7.0 Tesla. Magnetic resonance in medicine: official journal of the Society of Magnetic Resonance in Medicine/Society of Magnetic Resonance in Medicine. 2013; 69(1):114–126.
24. Yarnykh VL. Actual flip-angle imaging in the pulsed steady state: a method for rapid three-dimensional mapping of the transmitted radiofrequency field. Magnetic resonance in medicine: official journal of the Society of Magnetic Resonance in Medicine/Society of Magnetic Resonance in Medicine. 2007; 57(1):192–200.

25. Li X, Metzger GJ. Feasibility of measuring prostate perfusion with arterial spin labeling. NMR in biomedicine. 2013; 26(1):51–57. [PubMed: 22674425]
26. Li X, Sarkar SN, Purdy DE, Spence JS, Haley RW, Briggs RW. Anteroposterior perfusion heterogeneity in human hippocampus measured by arterial spin labeling MRI. NMR in biomedicine. 2013; 26(6):613–621. [PubMed: 23420779]
27. Buxton RB, Frank LR, Wong EC, Siewert B, Warach S, Edelman RR. A general kinetic model for quantitative perfusion imaging with arterial spin labeling. Magnetic resonance in medicine: official journal of the Society of Magnetic Resonance in Medicine/Society of Magnetic Resonance in Medicine. 1998; 40(3):383–396.
28. Bjornerud A, Johansson LO, Briley-Saebo K, Ahlstrom HK. Assessment of T1 and T2* effects in vivo and ex vivo using iron oxide nanoparticles in steady state--dependence on blood volume and water exchange. Magnetic resonance in medicine: official journal of the Society of Magnetic Resonance in Medicine/Society of Magnetic Resonance in Medicine. 2002; 47(3):461–471.
29. Buxton RB. Quantifying CBF with arterial spin labeling. J Magn Reson Imaging. 2005; 22(6):723–726. [PubMed: 16261574]
30. Parkes LM. Quantification of cerebral perfusion using arterial spin labeling: two-compartment models. J Magn Reson Imaging. 2005; 22(6):732–736. [PubMed: 16267854]
31. Dietrich O, Raya JG, Reeder SB, Reiser MF, Schoenberg SO. Measurement of signal-to-noise ratios in MR images: influence of multichannel coils, parallel imaging, and reconstruction filters. Journal of magnetic resonance imaging: JMRI. 2007; 26(2):375–385. [PubMed: 17622966]
32. Gillis KA, McComb C, Foster JE, Taylor AH, Patel RK, Morris ST, Jardine AG, Schneider MP, Roditi GH, Delles C, Mark PB. Inter-study reproducibility of arterial spin labelling magnetic resonance imaging for measurement of renal perfusion in healthy volunteers at 3 Tesla. BMC Nephrol. 2014; 15:23. [PubMed: 24484613]
33. Martirosian P, Klose U, Mader I, Schick F. FAIR true-FISP perfusion imaging of the kidneys. Magnetic resonance in medicine: official journal of the Society of Magnetic Resonance in Medicine/Society of Magnetic Resonance in Medicine. 2004; 51(2):353–361.
34. Robson PM, Madhuranthakam AJ, Dai W, Pedrosa I, Rofsky NM, Alsop DC. Strategies for reducing respiratory motion artifacts in renal perfusion imaging with arterial spin labeling. Magnetic resonance in medicine: official journal of the Society of Magnetic Resonance in Medicine/Society of Magnetic Resonance in Medicine. 2009; 61(6):1374–1387.
35. Erturk, MA., Raaijmakers, AJ., Adriany, G., Ugurbil, K., Metzger, GJ. Magnetic resonance in medicine: official journal of the Society of Magnetic Resonance in Medicine. Society of Magnetic Resonance in Medicine; 2016. A 16-channel combined loop-dipole transceiver array for 7 Tesla body MRI.
36. Erturk MA, Raaijmakers AJE, Adriany G, Tian J, Van de Moortele PF, Van den Berg CAT, Klomp DWJ, Vaughan JT, Ugurbil K, Metzger G. Comparison of 16-channel Stripline and 10-channel Fractionated Dipole Transceive Arrays for Body Imaging at 7T. Proc Intl Soc Mag Reson Med. 2015; 23:3122.
37. Zelinski AC, Wald LL, Setsompop K, Alagappan V, Gagoski BA, Goyal VK, Adalsteinsson E. Fast slice-selective radio-frequency excitation pulses for mitigating B+1 inhomogeneity in the human brain at 7 Tesla. Magnetic resonance in medicine: official journal of the Society of Magnetic Resonance in Medicine/Society of Magnetic Resonance in Medicine. 2008; 59(6):1355–1364.

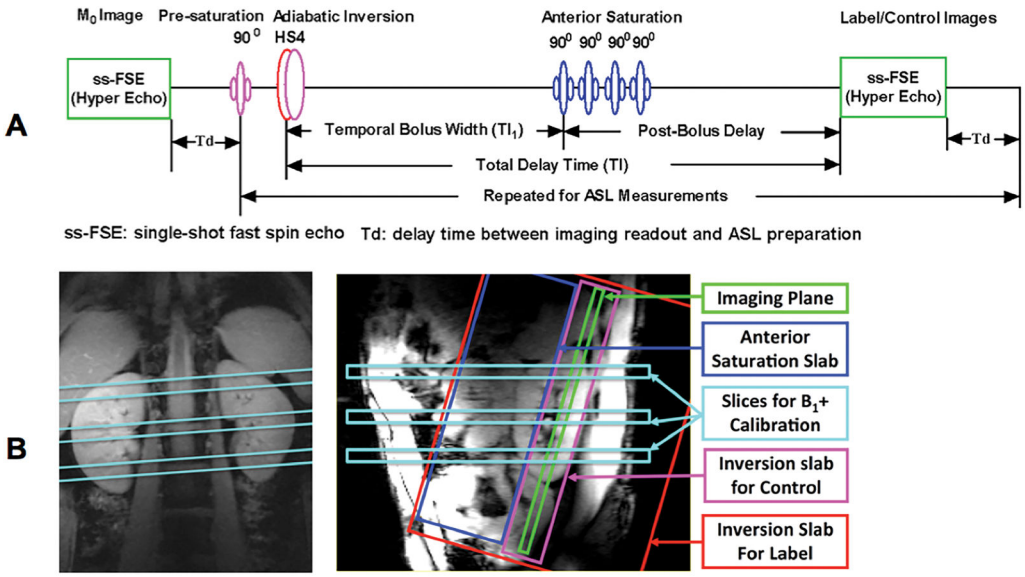

Figure 1.

Sequence diagram for renal perfusion imaging at 7T (A) and illustration of relative spatial positions of RF pulses using color-coded elements (B).

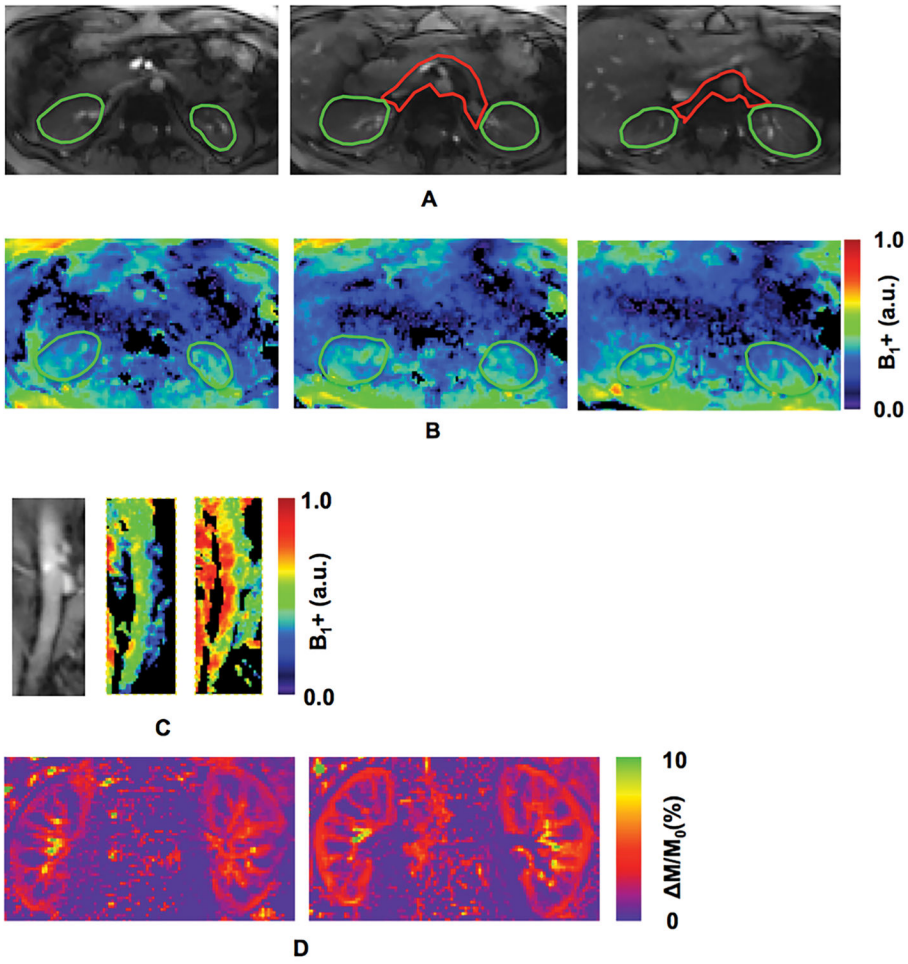

Figure 2.

Regions of interest (ROIs) for B_1^+ shimming, relative B_1^+ maps and normalized perfusion-weighted images from one volunteer: (A) ROIs for B_1^+ shimming in kidneys (green) and feeding arteries (red); (B) relative B_1^+ maps with B_1^+ optimization targeted to kidney regions only; (C) the anatomic image of descending aorta (C-left), and relative B_1^+ maps (C-middle) within the descending aorta after B_1+ shimming with the combined ROIs (green plus red ROIs in (A)) and (C-right) a smaller local ROI (red in (A)); and (D) normalized perfusion-weighted images using a single B_1^+ shimming solution optimized for both kidneys and the feeding arteries (D-left), and two dynamically applied B_1^+ shimming solutions separately optimized for kidneys and feeding arteries (D-right).

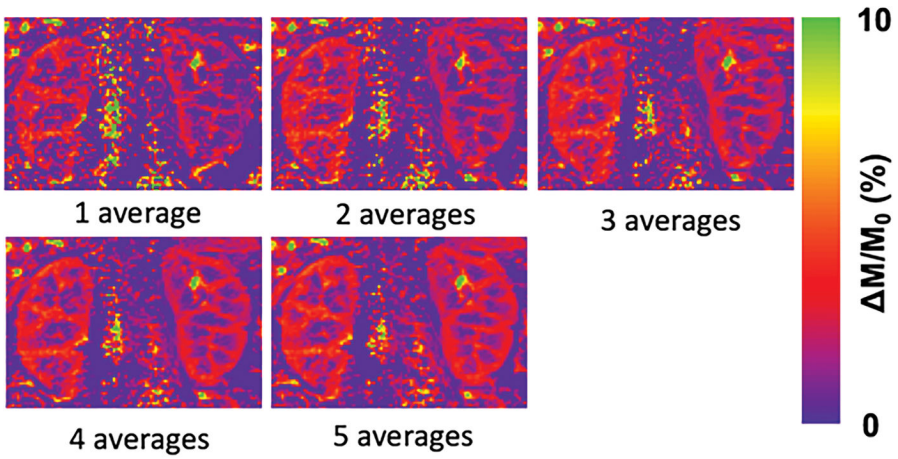

Figure 3.
One volunteer's normalized perfusion-weighted images obtained using a 1.5 s post-bolus delay with 1, 2, 3, 4 and 5 averages.

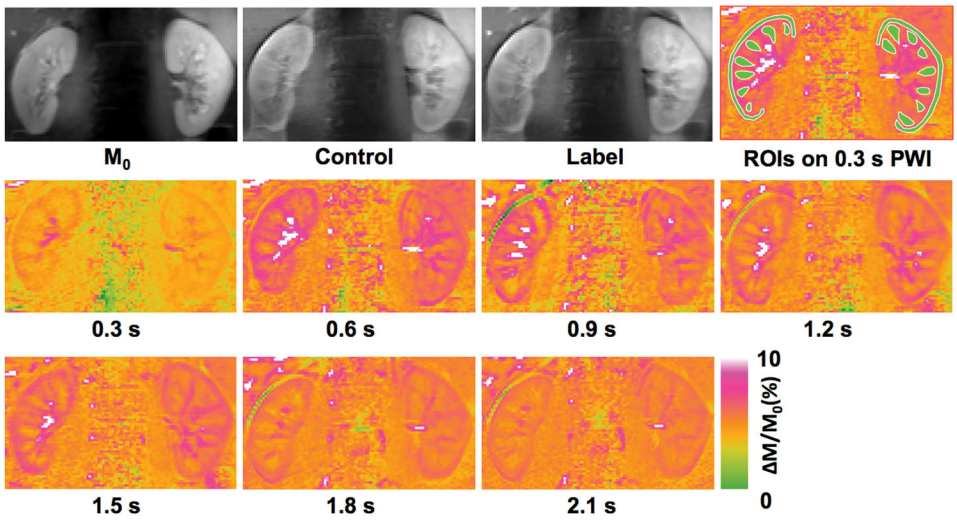

Figure 4.

Perfusion imaging results of one volunteer from the multi-delay study: M_0, control and label images, regions of interests for dynamic perfusion signal measurements (overlaid on normalized perfusion-weighted images acquired using a 0.6 s total delay), and normalized perfusion-weighted images acquired using 0.3, 0.6, 0.9, 1.2, 1.5, 1.8, and 2.1 s delays.

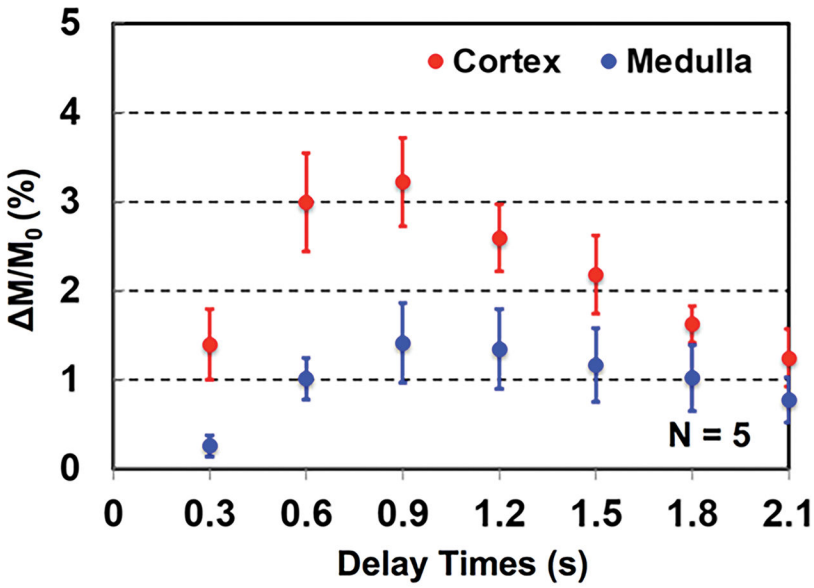

Figure 5.

Group means of normalized perfusion-weighted image signals from five subjects using 0.3, 0.6, 0.9, 1.2, 1.5, 1.8, and 2.1 s total delay times. Error bars represent the standard deviation.

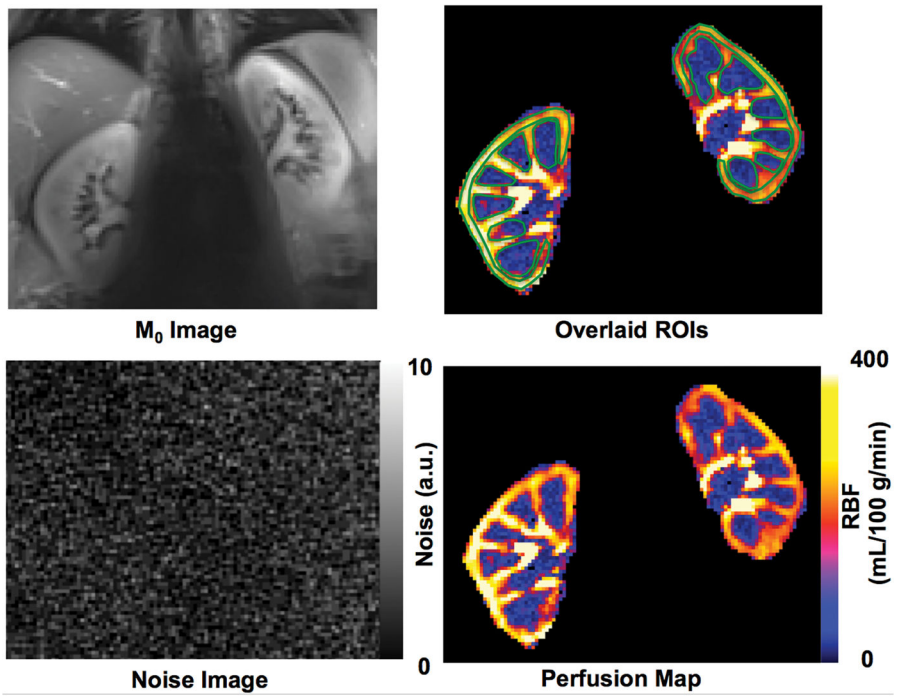

Figure 6.

Quantitative renal perfusion imaging study results using the single-subtraction approach from one volunteer: (A) M_0 image, (B) ROIs overlaid on renal blood flow (RBF) map for RBF estimation in the cortex and medulla, (C) noise image, and (D) RBF map.

Table 1

Arterial transit time (ATT), temporal bolus width and renal blood flow (RBF, mL/100 g/min) for renal cortex and medulla from the multi-delay perfusion study.

Subject No.	Cortex			Medulla		
	ATT	Temporal Bolus Width	RBF	ATT	Temporal Bolus Width	RBF
1	115.2	780.3	289.1	187.5	857.4	75.1
2	79.2	646.8	357.9	253.3	727.1	132.0
3	115.8	645.5	332.3	183.2	835.9	119.9
4	147.3	775.7	295.2	202.6	851.2	136.7
5	93.2	663.8	271.6	207.4	714.6	98.4
Mean	110.1	702.4	309.2	206.8	797.2	112.4
Standard Deviation	25.9	69.4	35.1	27.9	70.3	25.6

Table 2

Renal blood flow (RBF, mL/100 g/min), spatial signal-to-noise ratio (sSNR), temporal signal-to-noise ratio (tSNR), and p values of the comparisons between the measurements using four averages and those using two and three averages for renal cortex and medulla from the single-subtraction perfusion study with seven subjects*.

	Averages	RBF	sSNR	tSNR	p Values		
					RBF	sSNR	tSNR
Cortex	2	290.2 (26.0)	2.6 (0.4)	1.7 (0.5)	0.04	<0.01	<0.01
	3	306.1 (26.3)	3.4 (0.5)	2.1 (0.6)	0.31	<0.01	<0.01
	4	303.3 (31.8)	3.8 (0.7)	2.4 (0.6)	-	-	-
Medulla	2	87.6 (13.9)	1.7 (0.3)	1.0 (0.1)	0.02	<0.01	<0.01
	3	90.5 (13.4)	2.1 (0.4)	1.3 (0.1)	0.60	<0.01	0.01
	4	91.3 (15.2)	2.2 (0.6)	1.4 (0.2)	-	-	-

*The measurements of RBF, sSNR and tSNR are presented in the form of mean (standard deviation).